OncoTargets and Therapy

Dovepress
open access to scientific and medical research

Open Access Full Text Article

ORIGINAL RESEARCH

Elevated Levels of circRUNX1 in Colorectal Cancer Promote Cell Growth and Metastasis via miR-145-5p/IGF1 Signalling

This article was published in the following Dove Press journal:
OncoTargets and Therapy

Zhi-Lei Chen
Xiang-Nan Li
Chun-Xiang Ye
Hong-Yu Chen
Zhen-Jun Wang

Department of General Surgery, Beijing Chao-Yang Hospital, Capital Medical University, Beijing 10020, People's Republic of China

Background: Emerging evidence suggests that circular RNAs (circRNAs) are vital regulators in a range of cancers. "miRNA sponge" is the most reported role played by circRNAs in many tumors. The insulin-like growth factor (IGF) 1 pathway plays a key role in the development and progression of many cancers, including colorectal cancer (CRC). The aim of the study is to establish the potential clinical value and driving molecular mechanisms of circRNAs in CRC.

Materials and Methods: Real-time quantitative RT-PCR (qRT-PCR) was performed to measure the circRUNX1 expression in 52 tissue samples from CRC patients. We verified the tumor promotor role of circRUNX1 in cell-based in vitro and in vivo assays. Human growth factor array was used to identify circRUNX1-regulated signaling pathways. We then used a double luciferase reporter assay and RNA fluorescence in situ hybridization to identify the downstream miR-145-5p of circRUNX1. Furthermore, we performed Western blotting and biological function assays to demonstrate if the circRUNX1/miR-145-5p/IGF1 axis is responsible for the proliferation of CRC cells and promotes CRC development.

Results: By performing qRT-PCR from CRC tissues and paired adjacent normal mucosa tissues, we identified that circRUNX1 expression was significantly upregulated in CRC tissues and positively related with lymph node metastasis, distant metastasis and advanced tumor-node-metastasis tumor stage in patients. Functionally, circRUNX1 knockdown inhibited cell proliferation and migration and promoted apoptosis, whereas its overexpression exerted opposite effects. In vivo, circRUNX1 promoted tumor growth and metastasis. Mechanically, circRUNX1 shared miRNA response elements with IGF1. circRUNX1 competitively bound to miR-145-5p and prevented miR-145-5p from decreasing the expression of IGF1, which facilitated tumor growth.

Conclusion: Our studies verified that circRUNX1 functions as a tumor promotor in CRC cells by targeting the miR-145-5p/IGF1 signaling pathway and may have potential use as a prognostic indicator and therapeutic target in CRC patients.

Keywords: colorectal cancer, circRNAs, circRUNX1, human growth factor array, IGF1, tumor promotor, miR-145-5p

Introduction

Colorectal cancer (CRC) is the third leading cause of cancer-related death in the world, accounting for nearly 9% of cancer cases.[1,2] Although classical pharmacological treatment and surgery strategies have improved, no effective target therapy has been validated in CRC. Therefore, it is essential to identify more efficient molecular targets and new potential biomarkers for CRC therapy and monitoring.

Correspondence: Zhen-Jun Wang
Email drzhenjun@163.com

submit your manuscript | www.dovepress.com
DovePress
http://doi.org/10.2147/OTT.S254133

Several novel therapeutic agents for CRC have been investigated in recent years, especially noncoding RNAs (ncRNAs).[3,4] circRNA has emerged as a new noncoding RNA which is vital in tumor initiation and development.[5,6] Compared with the traditional linear RNA, circRNA is characterized by a covalently closed loop without terminal 5′ caps and 3′ polyadenylated tails.[7] Although circRNAs are expressed at low levels, they are naturally resistant to degradation by exonucleases and have long half-lives.[8] Previous studies have verified that circRNAs participate in various cell biological activities, including RNA binding protein regulators, miRNA-binding sponges and protein translation templates.[9,10] Although enormous circRNAs have been identified by RNA sequencing, little is known regarding their biological function in the pathogenesis of CRC.

IGF1 is a circulating endocrine hormone that is a major regulator of growth and metabolism.[11] It is therefore not surprising that transcriptional changes in IGF1 can induce cancer development and progression.[12,13] Many studies have shown the ability of the IGF1 pathway to promote colorectal tumorigenesis and metastasis.[14,15] IGF1 is targeted by 11 miRNAs including miR-145-5p, and miR-145-5p has been reported to function as a tumor suppressor in CRC. Downregulation of IGF1 levels can inhibit tumor growth, and has been considered as an attractive strategy for potential treatment of CRC patients.

In our study, we identified circRUNX1 (hsa_circ_0002360), which derived from the exon region of the *RUNX1* gene, is significantly upregulated in CRC tissues. Further analyses have indicated that circRUNX1 acts as a competing endogenous RNA (ceRNA) for miR-145-5p to upregulate IGF1, which subsequently contributes to tumorigenesis and progression in CRC. Our results indicated that circRUNX1 can be seen as a novel biomarker of and potential therapeutic target for CRC.

Materials and Methods

Patients and Samples

Fifty-two paired samples of tumor tissues and adjacent normal mucosal tissues were obtained from surgical resection of CRC patients without preoperative chemoradiotherapy at Beijing Chao-Yang Hospital (Beijing, China) during 2018 and 2019. All resected fresh tissues were immediately infiltrated in RNAlater (Invitrogen, Carlsbad, CA, USA) and stored at −80°C. All of the pathologic specimens were histologically verified by two pathologists independently. This project was approved by the Ethics Committee of Beijing Chao-Yang Hospital Affiliated to Capital Medical University and conducted in accordance with the Declaration of Helsinki. Written informed consent was obtained from all enrolled patients. Clinicopathologic features of patients are summarized in Table 1.

Cell Culture

All human CRC cells (SW480, SW620, HCT116, HT29, LoVo and RKO) were purchased from the American Type Culture Collection. Cells were tested negative for mycoplasma contamination before experiment. SW480, SW620, LoVo and RKO cells were cultured in Dulbecco's modified Eagle's medium (Biological Industries, Cromwell, CT, USA) with 10% FBS; HCT116 and HT29 cells were cultured in McCoy's 5A medium with 10% FBS. Cells were all cultured at 37°C with 5% CO_2.

RNA Extraction and Real-Time Quantitative RT-PCR

Total RNA was extracted from CRC tissues and cells with Trizol (Invitrogen). The cDNA of circRUNX1 was synthesized using reverse transcription PrimeScript™ RT Reagent Kit (Takara, Dalian, China). In order to measure the abundance of transcripts, qPCR of circRUNX1 was conducted using TB Green™ Premix Ex Taq™ II Kit (TaKaRa); 18S rRNA was utilized as an internal control. The $2^{-\Delta Ct}$ or $2^{-\Delta\Delta Ct}$ method was used to calculate the relative expression of RNA. All the primers in this study were expressed as follows: circRUNX1 forward: 5′-TCCCTGAACCACTCCACTGC-3′, reverse: 5′-GACTTGCGGTGGGTTTGTGA-3′; 18S rRNA forward: 5′-AAACGGCTACCACATCCA-3′, reverse: 5′-CACCAGACTTGCCCCTCCA-3′.

Transfection

Small interfering RNAs (siRNAs) which target the back-splice junction sequences of circRUNX1, miR-145-5p mimics, and their respective NC oligonucleotides were designed and synthesized from GenePharma (Shanghai, China). The oligonucleotides were transfected into CRC cells using Lipofectamine 3000 reagent (Invitrogen) at a final concentration of 75 nM. The sequences of oligonucleotides were as follows: si-circRUNX1#1: 5′-GAGUCAGAUGCAGGGGAAATT-3′; si-circRUNX1#2: 5′-AGAUGCAGGGGAAAAGCUUTT-3′; miR-145-5p: 5′-GUCCAGUUUUCCCAGGAAUCCCU-3′; negative control: 5′-UUCUCCGAACGUGUCACGUTT-3′.

Table 1 Correlation of circRUNX1 Expression with Clinicopathologic Features of CRC Patients

Clinicopathologic Features	Total (n = 52)	circRUNX1 Expression[a]		*p* value
		High	Low	
Age (yr)				
≥65	27	13 (48.1%)	14 (51.9%)	0.78
<65	25	13 (52.0%)	12 (48.0%)	
Gender				
Male	28	15 (53.6%)	13 (46.4%)	0.58
Female	24	11 (45.8%)	13 (54.2%)	
Tumor size (cm)				
≥5	25	14 (56.0%)	11 (44.0%)	0.41
<5	27	12 (44.4%)	15 (55.6%)	
Differentiation				
Poor	7	4 (57.1%)	3 (42.9%)	1.00
High	45	22 (48.9%)	23 (51.1%)	
Tumor site				
Rectum	17	9 (52.9%)	8 (47.1%)	0.77
Colon	35	17 (48.6%)	18 (51.4%)	
Depth of invasion				
T3/T4	45	21 (46.7%)	24 (53.3%)	0.42
T1/T2	7	5 (71.4%)	2 (28.6%)	
Lymph node metastasis				
N1/N2	21	15 (71.4%)	6 (28.6%)	0.01**
N0	31	11 (35.5%)	20 (64.5%)	
Distant metastasis				
M1	5	5 (100%)	0 (0%)	0.05*
M0	47	21 (44.7%)	26 (55.3%)	
TNM tumor stage				
III+ IV	22	16 (72.7%)	6 (27.3%)	0.01**
I+II	30	10 (33.3%)	20 (66.7%)	
Lymphovascular invasion				
Present	29	15 (51.7%)	14 (48.3%)	0.78
Absent	23	11 (47.8%)	12 (52.2%)	

Notes: *$p < 0.05$. **$p < 0.01$. [a]Using median expression level of circRUNX1 as cutoff.

circRUNX1-Expressing Lentivirus Preparation and Infection

Lentiviruses expressing circRUNX1 were purchased from Hanbio (Shanghai, China). For lentivirus constructs, the CDS (Coding sequence) of circRUNX1 was inserted into pHBLV-CMV-MCS-EF1-puro lentiviral vectors (Hanbio). The constructed vectors were packaged into lentiviruses. To establish stable cell lines, CRC cells were infected with lentiviruses with or without circRUNX1 at MOI 1 in the presence of 6 μg/mL polybrene. Approximately 48 h after infection, the medium was changed, and puromycin was added for selection of stable transfected cells. Puromycin-resistant colonies were selected for 1–2 weeks and then expanded. Gene modification via lentiviral delivery was confirmed by qRT-PCR.

RNA Fish

The circRUNX1 probe sequence, which was administrated by Cy3-labeled at the 5′ end, was 5′-GTCAGAGTGA AGCTTTTCCCCTGCATCTGACTCTGAGGCT-3′. The 5′ FAM-labeled miR-145-5p probe sequence was 5′-AGGGA +TTCCTGGGAAAAC+TGGAC-3′. These probes were all synthesized by GenePharma. FISH staining was performed according to the manufacturer's instructions (GenePharma). DAPI was used to stain the cell nuclei. A confocal laser scanning microscope (TCS SP8; Leica, Wetzlar, Germany) was used to observe the subcellular distribution of circRUNX1 and miR-145-5p in CRC cells.

Colony-Formation Assay

Briefly, 10^3 CRC cells were resuspended and plated into each well of a six-well plate and incubated at 37°C for 2 weeks. The cell colonies were observed after fixation with 4% paraformaldehyde for 20 min and staining with 0.1% crystal violet for 20 min. Pictures were acquired soon after staining, and colonies were counted and analyzed.

CCK-8 Assay

Cell proliferation assay was tested with the CCK-8 kit (Dojindo Laboratories, Kumamoto, Japan). Approximately 10^3 cells were resuspended and plated into 96-well plates and cultured for different time periods, respectively (0, 24, 48, 72 or 96h). Then each well was added with 10 μL CCK-8 reagent. After incubation for 2 h, absorbance at 450 nM was assessed using a microtiter plate reader (Thermo Fisher Scientific, Waltham, MA, USA). The data of the OD-measuring were used to reflect cell proliferation rates. Cells in each group were performed for five replicates.

Transwell Assay

For invasion and migration assay, cells in suspension (serum-free medium) were seeded into migration chambers (Corning, NY, USA) present in the insert of a 24-well culture plate. Matrigel (Corning) was prepared at the bottom of the PC Membrane in advance for the invasion assays. Medium containing 20% fetal bovine serum was

added to the lower chambers. After incubation at 37°C for 24 h or 48 h (for migration assays or invasion assays), the cells in the upper chambers were removed, and paraformaldehyde was used to fix the remaining cells. Cells in five random 100× fields were counted to calculate the invasion and migration cell number using a Leica DM4000B microscope (Leica).

Flow Cytometry Analysis

Cell apoptosis and cell cycle assays were performed using flow cytometry analysis (BD Biosciences, San Jose, CA, USA). For apoptosis experiments, CRC cells were collected and re-suspended with 500 μL binding buffer. FITC and PI (KeyGen Biotech, Nanjing, China) were added and incubated for 15 min at room temperature in the dark. Samples were instantly analyzed by flow cytometry. And for cell cycle assay, CRC cells were collected and mixed with 75% ethanol at 4°C overnight. Cells were labeled with PI/RNase Staining Buffer for 30 min before detection. The data were analyzed by flow cytometer FACSCalibur (De Novo Software, Los Angeles, CA, USA).

Mouse Xenograft Model

All animal studies were approved by the Committee on the Ethics of Animal Experiments of Beijing Chao-Yang Hospital Capital Medical University, and were performed in compliance with the Animal Protection Law of the People's Republic of China-2009 for experimental animals. Male BALB/c nude mice aged 6–8 weeks were housed under standard conditions and conformed to the Guide for the Care. 2×10^6 HCT116 cells (circRUNX1 over-expression plasmid or mock vector) were subcutaneously inoculated into the dorsal flanks of mice (eight in each group). The volume of tumors was evaluated every 3 days by the following formula: (length × width^2)/2. 15 days later, mice were killed and tumors were measured.

In the experiments of liver metastases, 2×10^6 cells were intravenously injected into the spleen of mice (four in each group). 30 days later, the livers and spleens were excised after the mice were killed, and the numbers of liver metastases nodules were counted visually. All of the pathologic specimens were subsequently confirmed via histological analysis.

Human Growth Factor Array

Human Growth Factor Array Q1 (RayBiotech, Norcross, GA, USA) was used for detection. SW480 cells were resuspended and plated in 100-mm dishes and incubated at 37°C for 72 h. Conditioned proteins were collected and incubated with antibody microarrays according to the manufacturer's instructions. Images were obtained with a chemoluminescent imaging system and densitometry analysis was detected using ImageJ software.

Western Blotting Analysis

Total protein of CRC cell lines was extracted by RIPA lysis buffer (Solarbio, Beijing, China) and the concentration was measured using BCA Protein assay kit (Beyotime, China). Equal amounts of total protein (30 μg) were separated by 12% SDS–PAGE and transferred onto PVDF membranes. After blocking with 5% BSA in TBST buffer for 2 h, the membranes were incubated with IGF1 antibody (1:1000 dilution; 133542; abcam, Cambridge, UK), or β-actin (1:5000 dilution; 66009-1-lg; Proteintech, Chicago, IL, USA) overnight at 4°C. Afterwards, the membranes were incubated with a corresponding HRP-labelled secondary antibody (1:5000, Lablead, Beijing, China) for 1 h at room temperature. Finally, the blots were visualized using an enhanced chemiluminescent kit (Beyotime, China). Quantification of the individual protein bands was performed by densitometry using ImageJ software.

Bioinformatics Analysis

We used bioinformatics algorithms Circular RNA Interactome (https://circinteractome.nia.nih.gov/index.html) to predict the target miRNAs of circRUNX1. The target proteins of miRNAs were predicted using Target Scan (http://www.targetscan.org). We chose 7mer-M8, 7mer-A1 or 8mer site type for further analysis.

Dual-Luciferase Reporter Assay

The full-length circRUNX1 or the 3′ untranslated region (UTR) of IGF1 sequences containing mutant or wild-type miR-145-5p binding sites were synthesized and cloned into psiCHECK-2 plasmid (Promega, Madison, WI, USA). The mutated or wild-type plasmids were cotransfected with miR-145-5p mimics or mimics NC into HEK293 cells using Lipofectamine 3000 reagent (Invitrogen). 48 hours after transfection, the luciferase activity was measured with a dual-luciferase reporter assay system (Promega). Independent experiments were conducted in triplicate.

Statistical Analysis

All the analyses were performed using SPSS 23.0 (IBM, SPSS, Chicago, IL, USA). GraphPad Prism 7.0 (GraphPad

Software, La Jolla, CA, USA) was used to produce all the figures. Differences between groups were analyzed using chi-square test, Student's *t* test, Wilcoxon signed rank test and one-way analysis of variance, as appropriate. Quantitative data were listed as mean ± SD. A *p* value < 0.05 was considered statistically significant.

Results

Expression of circRUNX1 Is Significantly Upregulated in CRC Tissues and Correlated with Tumor Progression

In the preliminary experiments, we detected hundreds of potential circRNAs using high-throughput RNA sequencing in four paired CRC tissues.[16] Finally, we found that circRUNX1 (hsa_circ_0002360) was significantly upregulated in the CRC tissues compared with paired normal mucosal tissues. According to circBase databases, circRUNX1 is derived from exons 2 and 3 of RUNX1, with a spliced mature sequence length of 297 base pairs (bp) (Figure 1A). To observe the subcellular distribution of circRUNX1 in CRC cells, RNA FISH was performed using SW480 cells, indicating that circRUNX1 was mostly located in the cytoplasm (Figure 1B). In order to confirm the upregulated expression of circRUNX1 in large samples of CRC patients, we detected another 52 paired CRC tissues by qRT-PCR (Figure 2A and B). Results showed that the expression of circRUNX1 was significantly upregulated in CRC tissues compared to matched normal tissues ($p < 0.001$). We divided the 52 CRC patients into low- and high-expression groups using the median expression level of circRUNX1 as a cutoff value (Figure 2C). Statistical analyses indicated that the level of circRUNX1 was significantly correlated with lymph node metastasis ($p = 0.01$), distant metastasis ($p = 0.05$) and TNM tumor stage ($p = 0.01$) (Table 1). In summary, these results suggest that circRUNX1 upregulation is common in CRC and its regulation is associated with later clinical stage (Figure 2D).

circRUNX1 Modulates Cell Proliferation, Cell Apoptosis, Cell Cycle, and Cell Migration in vitro

In order to explore the biological significance of circRUNX1 in CRC progression, gain-of-function and loss-of-function experiments were performed. Based on the different expression of circRUNX1 in several CRC cell lines (Figure 3A), we decided to silence circRUNX1 expression in SW480 and HCT116 cells. si-circRUNX1#1 and si-circRUNX1#2 targeting the back-splice region of circRUNX1 were designed (Figure 3B) and qRT-PCR showed that si-circRUNX1#1 significantly decreased circRUNX1 level similarly to si-circRUNX1#2. For the higher efficiency of interference, si-circRUNX1#1 was chosen for subsequent experiments. CCK-8 and colony formation assays indicated that downregulation of circRUNX1 significantly inhibited cell proliferation and colony formation (Figure 3C and D). Flow cytometry was performed to evaluate the effect of circRUNX1 on cell cycle or apoptosis progression. Silence of circRUNX1 inhibited cell cycle progression in SW480 and HCT116 cells compared with the NC group (Figure 3E). Furthermore, circRUNX1 siRNA

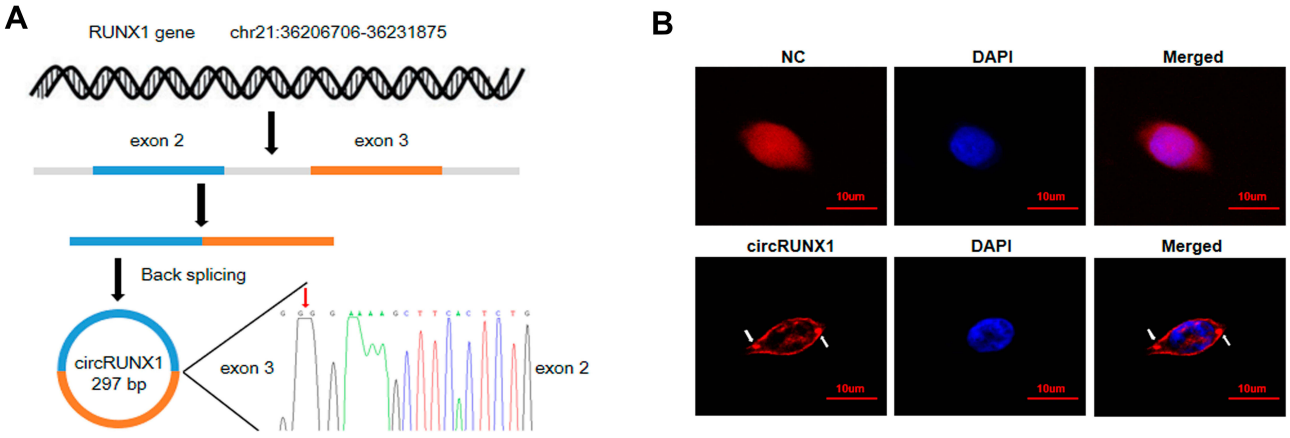

Figure 1 Biogenesis, Sanger sequencing and subcellular distribution of circRUNX1. (**A**) circRUNX1 is derived from exons 2 and 3 of RUNX1 gene by back splicing. The back-splice junction sequences of circRUNX1 were confirmed by Sanger sequencing. We use the red arrow to mark the junction site. (**B**) The subcellular distribution of circRUNX1 was identified using RNA FISH in SW480 cells. Red (Cy3-labeled probe) indicates the circRUNX1 or negative control (NC). DAPI indicates the nucleus. Scale bars = 10 μm.

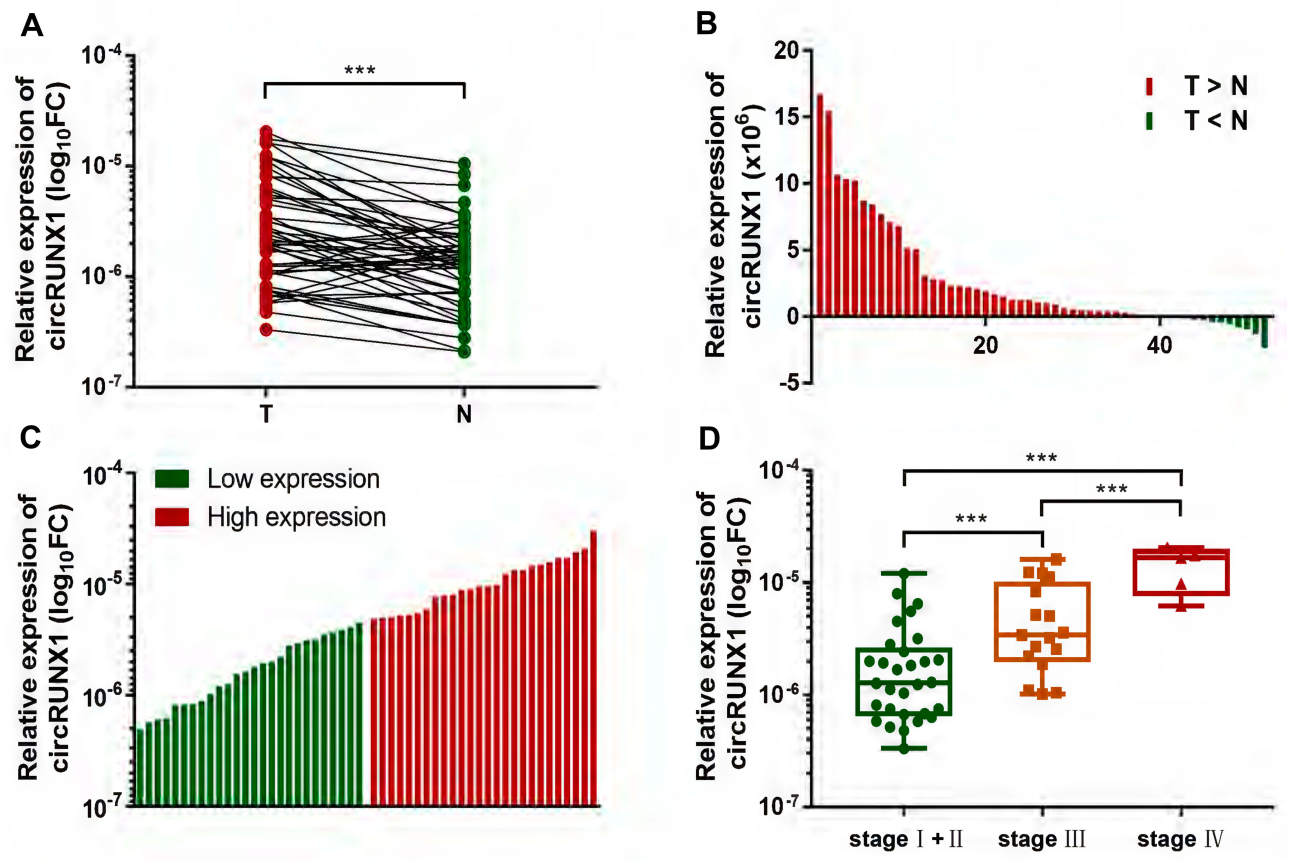

Figure 2 circRUNX1 was upregulated in CRC tissues and correlated with tumor progression. (**A**) qRT-PCR for circRUNX1 in 52 pairs of CRC and matched adjacent normal mucosal tissues showed that circRUNX1 was significantly upregulated. (**B**) 69.2% (36 of 52) of the CRC tissues presented increased expression of circRUNX1 compared to matched normal tissues. (**C**) Using the median expression level of circRUNX1 as a cutoff value, the 52 CRC tissues were divided into low and high expression groups. (**D**) The level of circRUNX1 showed an increased trend with TNM tumor stage. All data are presented as the means ± SD of at least three independent experiments. ***$p < 0.001$. T, tumor tissues; N, normal tissues.

promoted apoptosis (Figure 3F). Transwell assays, including migration and invasion, were performed to determine repression of cell migration and invasion by downregulating circRUNX1 (Figure 3G). We developed SW480 or HCT116 cells with circRUNX1 stably overexpressed using pHBLV-CMV-MCS-EF1-puro lentiviral vectors (Figure 4A). Overexpression of circRUNX1 showed an opposite role in cell proliferation, cell apoptosis, cell cycle, and cell migration (Figure 4B–F).

Intratumoral Overexpression of circRUNX1 Enhances CRC Growth and Metastasis in vivo

A nude mice xenograft model was used to identify the effect of circRUNX1 on tumor growth in vivo. HCT116 cells with mock vector or circRUNX1 were subcutaneously injected into each mice. After 15 days of HCT116 cell injection, the tumor volumes were analyzed. We found that tumor volumes were significantly larger in the circRUNX1 than those in the NC groups (Figure 5A–C). Moreover, the effect of circRUNX1 overexpression upon tumor metastasis in vivo was also investigated. A intrasplenic injection model of HCT116 cells treated with mock vector or circRUNX1 was developed, then the animals were killed after 30 days of tumor cell injection when they were thin, arch-backed and acting dilatorily. HCT116 cells with circRUNX1 overexpression had more liver metastasis (4/4) than the NC groups (2/4) (Figure 5E). All samples containing subcutaneous tumor tissues and liver metastasis tissues were confirmed by HE staining (Figure 5D and F). On this basis, we identified circRUNX1 as a promoting factor of CRC progression in vivo.

circRUNX1 Facilitates Cell Proliferation by Targeting IGF1

In order to identify the factors by which circRUNX1 promoted proliferation of CRC cell lines, an antibody-based

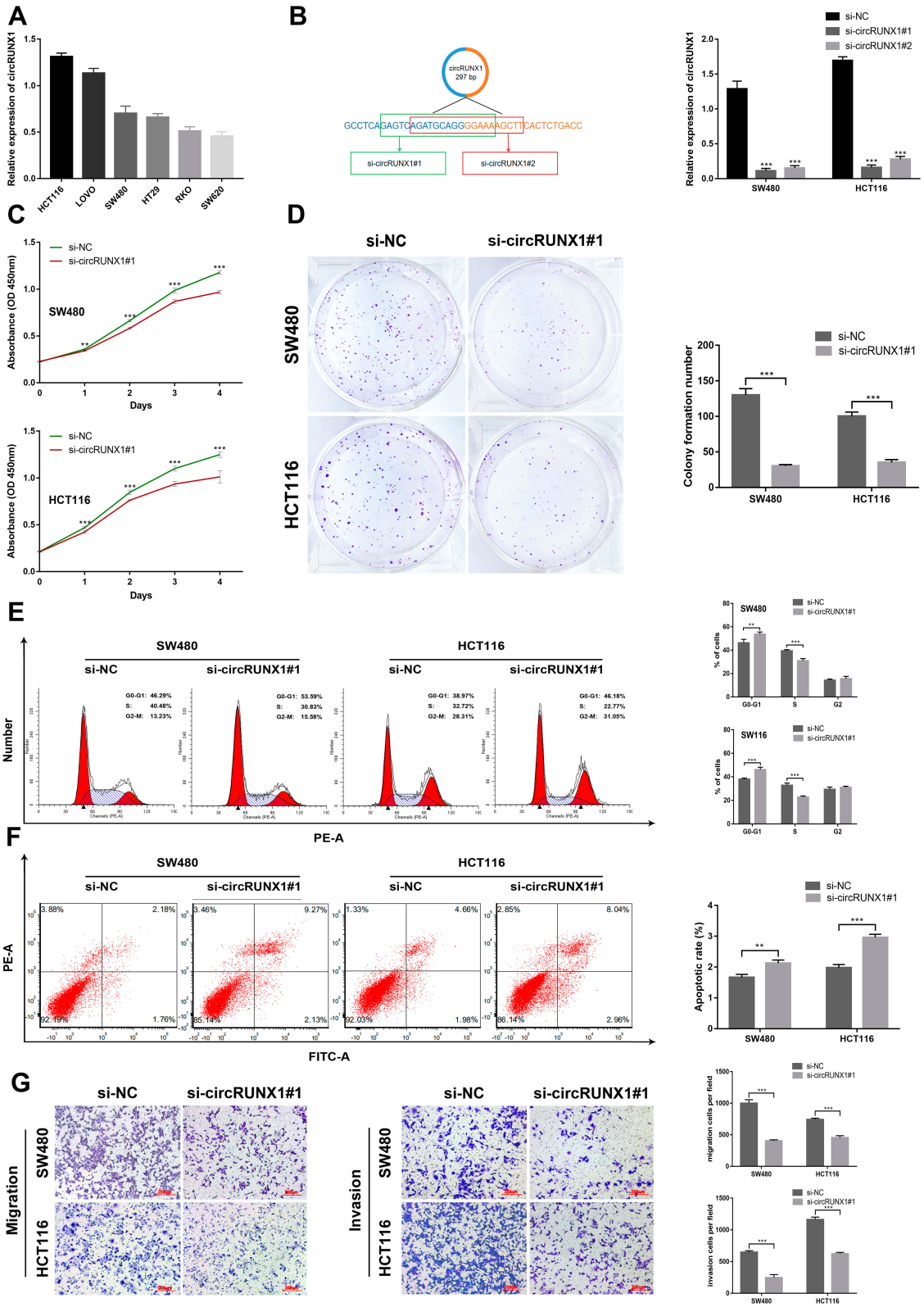

Figure 3 Silencing of circRUNX1 inhibits cell proliferation, cell cycle and cell migration and promoted apoptosis. (**A**) qRT-PCR was performed to verify the expression of circRUNX1 in CRC cell lines. (**B**) Expression of circRUNX1 in SW480 and HCT116 cells treated with circRUNX1 siRNA. (**C**) CCK8 assay assessed cell growth. (**D**) Colony formation assays were conducted in differently treated cells. (**E**) Flow cytometry was performed to indicate cell cycle. (**F**) Flow cytometry was performed to indicate cell apoptosis. The histogram displays the ratio of early apoptosis. (**G**) Transwell assays were used to evaluate the cell migration and invasive capability. Data are listed as means ± SD of at least three independent experiments. $^{**}p < 0.01$, $^{***}p < 0.001$. Scale bars = 200 μm.

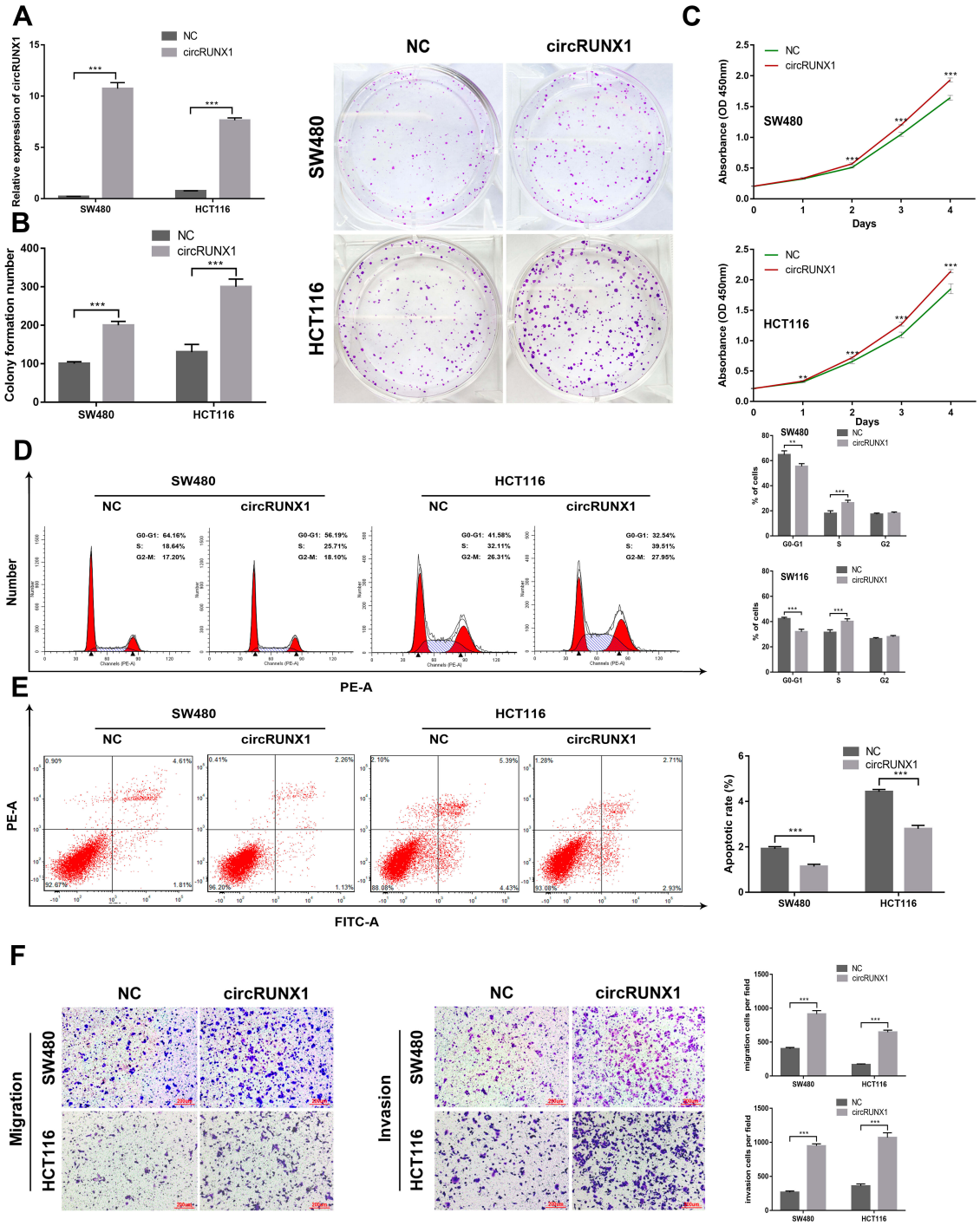

Figure 4 Overexpression of circRUNX1 promotes cell proliferation, cell cycle and cell migration and inhibited apoptosis. (**A**) Expression of circRUNX1 in SW480 and HCT116 cells after infection with circRUNX1 lentiviruses or negative control lentiviruses. (**B**) Colony formation assays were conducted in differently treated cells. (**C**) CCK8 assay assessed cell growth. (**D**) Flow cytometry was performed to indicate cell cycle. (**E**) Flow cytometry was performed to indicate cell apoptosis. The histogram displays the ratio of early apoptosis. (**F**) Transwell assays evaluated cell migration and invasive capability. Data are listed as means ± SD of at least three independent experiments. **$p < 0.01$, ***$p < 0.001$. Scale bars = 200 μm.

cytokine array that could detect 40 different growth factors and cytokines was performed to analyze the differences between circRUNX1 overexpression and control groups of SW480 cells. As demonstrated in Table 2, eight typical growth factors and cytokines, including bone morphogenetic protein (BMP) −5, IGF1, BMP-4, nerve growth factor receptor (NGFR), SCFR, growth hormone (GH), IGF binding protein (IGFBP) 6 and OPG, were significantly upregulated

in circRUNX1 overexpression groups, ≥1.5-fold versus control groups (Figure 6A). In another pair of experiments, we detected five decreased growth factors and cytokines between si-circRUNX1#1 and si-NC groups of SW480 cells; that is, IGF1, Insulin, OPG, transforming growth factor (TGF) α and EG-VEGF (Table 3, Figure 6B). The subsequent Venn analysis implied that IGF1 and OPG might be the target proteins of circRUNX1, which is involved in the proliferation of CRC (Figure 6C). Between the two molecules, IGF1 produced the more significant change and was confirmed to play an important role in CRC proliferation (Figure 6D). To validate our results that circRUNX1 regulated expression of IGF1, we detected IGF1 expression in HCT116 cells by Western blotting (Figure 6E). On this basis, we showed that there may be positive relationship between the expression level of circRUNX1 and IGF1.

circRUNX1 and IGF1 Act as ceRNAs in CRC Through Regulation of miR-145-5p

circRNAs act as an miRNA sponge to regulate gene expression. Bioinformatics algorithms Circular RNA Interactome was used to predict the potential target miRNAs of circRUNX1. Among these diverse miRNAs, miR-145-5p was reported to be the potential target of IGF1, with a site type of 7mer-M8 based on Target Scan.[17] To identify the interaction of circRUNX1 and miR-145-5p, and miR-145-5p and IGF1, luciferase reporter plasmids with mutant or wild-type circRUNX1 or IGF1 sequences were cotransfected with miR-145-5p mimics or mimics NC. Overexpression of miR-145-5p mimics markedly reduced luciferase activity to approximately 50% when compared with the NC (Figure 7A). FISH analysis showed that circRUNX1 and miR-145-5p colocalized in the cytoplasm (Figure 7B).

To further confirm that circRUNX1 can serve as a ceRNA to regulate IGF1 expression, we transfected SW480 and HCT116 cells with miR-145-5p mimics after overexpression of circRUNX1. miR-145-5p mimics markedly decreased IGF1, but it was rescued by circRUNX1 overexpression (Figure 7C). Cell proliferation assay was used to investigate the effect of miR-145-5p in CRC cells. Overexpression of miR-145-5p inhibited cell proliferation and overexpression of circRUNX1 rescued miR-145-5p-mimic-mediated suppression of cell proliferation (Figure 7D). These studies showed that circRUNX1 serves as a sponge for miR-145-5p to regulate IGF1 and promotes cell proliferation via the ceRNA mechanism in CRC cells (Figure 8).

Discussion

Recently, the regulatory potential of circRNAs in cancers has attracted great attention, especially using whole transcriptome

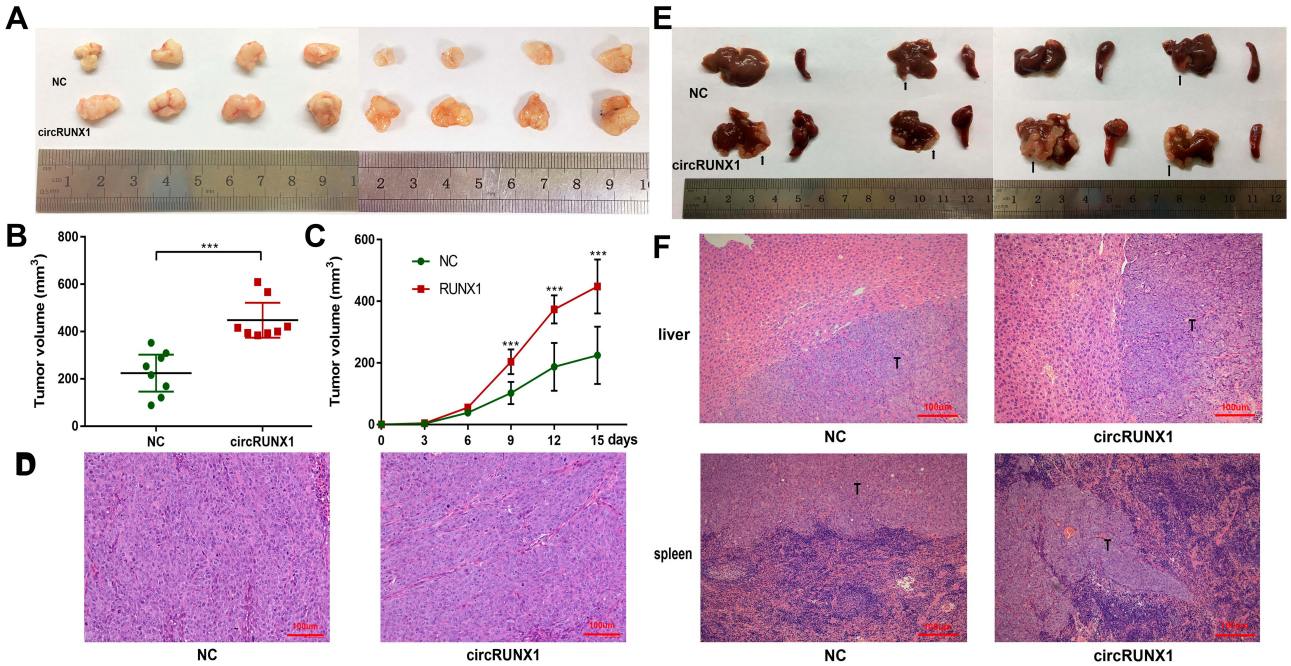

Figure 5 circRUNX1 promoted cell proliferation and metastasis in vivo. (**A**) Subcutaneous xenograft tumors isolated from nude mice. (**B**) Volumes of xenograft tumors are summarized. (**C**) Tumor volumes were monitored every 3 days for 15 days. (**D**) Representative images of HE-stained subcutaneous xenograft tumors. (**E**) Images of livers and spleens isolated from nude mice. The arrows show liver metastasis nodules. (**F**) Representative images of HE-stained liver metastasis nodules and spleen primary tumors. Data are listed as means ± SD. ***$p < 0.001$. Scale bars = 100 μm.

Table 2 Upregulated Proteins in circRUNX1 Overexpression Group and Control Group from Human Growth Factor Array

Growth Factors and Cytokines	AveExp. circRUNX1 Overexpression Group	AveExp. Control Group	Log_2FC	Fold Change
OPG	6.32	5.73	0.59	1.51
IGFBP-6	11.37	10.78	0.59	1.51
GH	8.08	7.24	0.84	1.79
SCFR	2.46	1.44	1.02	2.03
NGFR	3.50	1.79	1.71	3.27
BMP-4	5.41	2.80	2.61	6.11
IGF-1	6.09	2.46	3.63	12.38
BMP-5	4.55	0.00	4.55	23.43

Note: AveExp. Sample=Ave Log_2(protein concentration+1).

approaches.[18,19] In our preliminary experiment, we detected hundreds of potential circRNAs using high-throughput RNA sequencing in four paired CRC tissues. However, most of the circRNAs showed no clinicopathological significance when enlarging the patient sample. In our experiments, we identified circRUNX1 as a significantly upregulated circRNA and correlated with tumor progression in 52 CRC patients. Gain-of-function and loss-of-function studies demonstrated that circRUNX1 was related with cell proliferation, cell apoptosis, cell cycle, and cell migration.

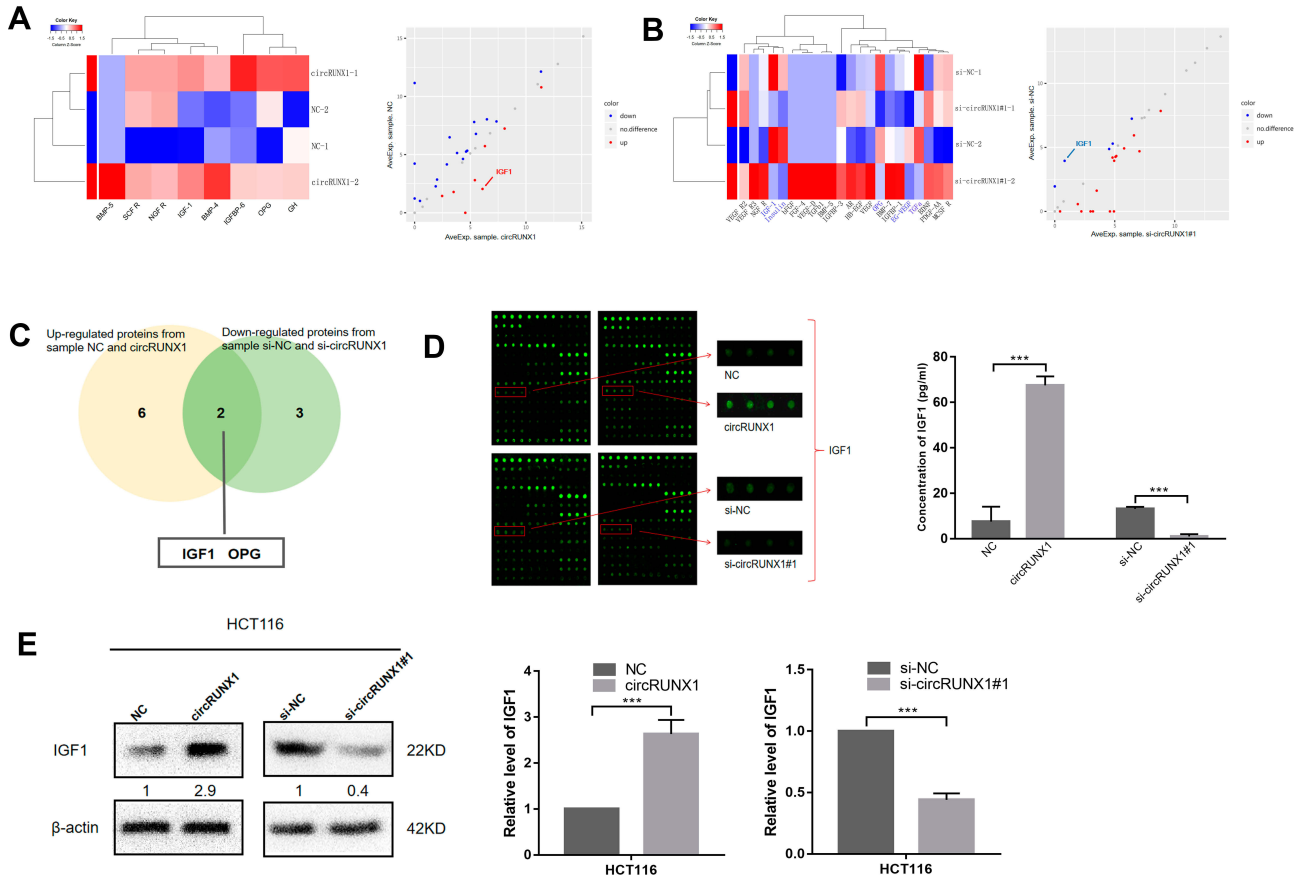

Figure 6 circRUNX1 facilitates cell proliferation by targeting IGF1 in CRC cell lines. (**A**) Heat map analyses and scatter plot showed eight upregulated proteins in circRUNX1 overexpression and control groups in SW480 cells with fold changes >1.5 and $p< 0.05$. (**B**) Heat map analyses and scatter plot showed five downregulated proteins in si-circRUNX1#1 and si-NC groups in SW480 cells with fold changes >1.5 and $p< 0.05$. (**C**) Venn analysis in eight upregulated and five downregulated proteins implied that IGF1 and OPG are target proteins of circRUNX1. (**D**) Representative images of growth factor antibody arrays: IGF1 produced the most significant change induced by circRUNX1. (**E**) The protein levels of IGF1 were detected through Western blotting after overexpression or silencing of circRUNX1 in HCT116 cells. Data are listed as means ± SD. ***$p< 0.001$.

Table 3 Downregulated Proteins in Si-circRUNX1#1 Group and Si-NC Group from Human Growth Factor Array

Growth Factors and Cytokines	AveExp. si-circRUNX1#1	AveExp. si-NC	Log_2FC	Fold Change
IGF1	0.79	3.82	−3.03	0.12
Insulin	0.00	1.95	−1.95	0.26
OPG	6.42	7.24	−0.82	0.57
TGFα	4.83	5.63	−0.80	0.57
EG-VEGF	4.26	4.87	−0.61	0.66

Note: AveExp. sample=Ave Log2(protein concentration+1).

Consistent with the above results, overexpression of circRUNX1 enhanced the proliferation and invasion of HCT116 cells in nude mouse models. All these findings support the oncogenic role of circRUNX1 in CRC tumorigenesis.

To better understand the functional mechanism of circRUNX1, human growth factor array was performed to identify the potential signaling pathways. Antibody-based cytokine arrays represent one of the high-throughput techniques which can detect multiple proteins simultaneously.[20] According to human growth factor array analysis, we found circRUNX1 modulates a number of growth factors known to promote CRC cell proliferation. Overexpression of circRUNX1 released high levels of BMP-5, IGF1, BMP-4, NGFR, SCFR, GH, IGFBP6 and OPG, while knockdown of circRUNX1 reduced expression of IGF1, insulin, OPG, TGFα and EG-VEGF. We

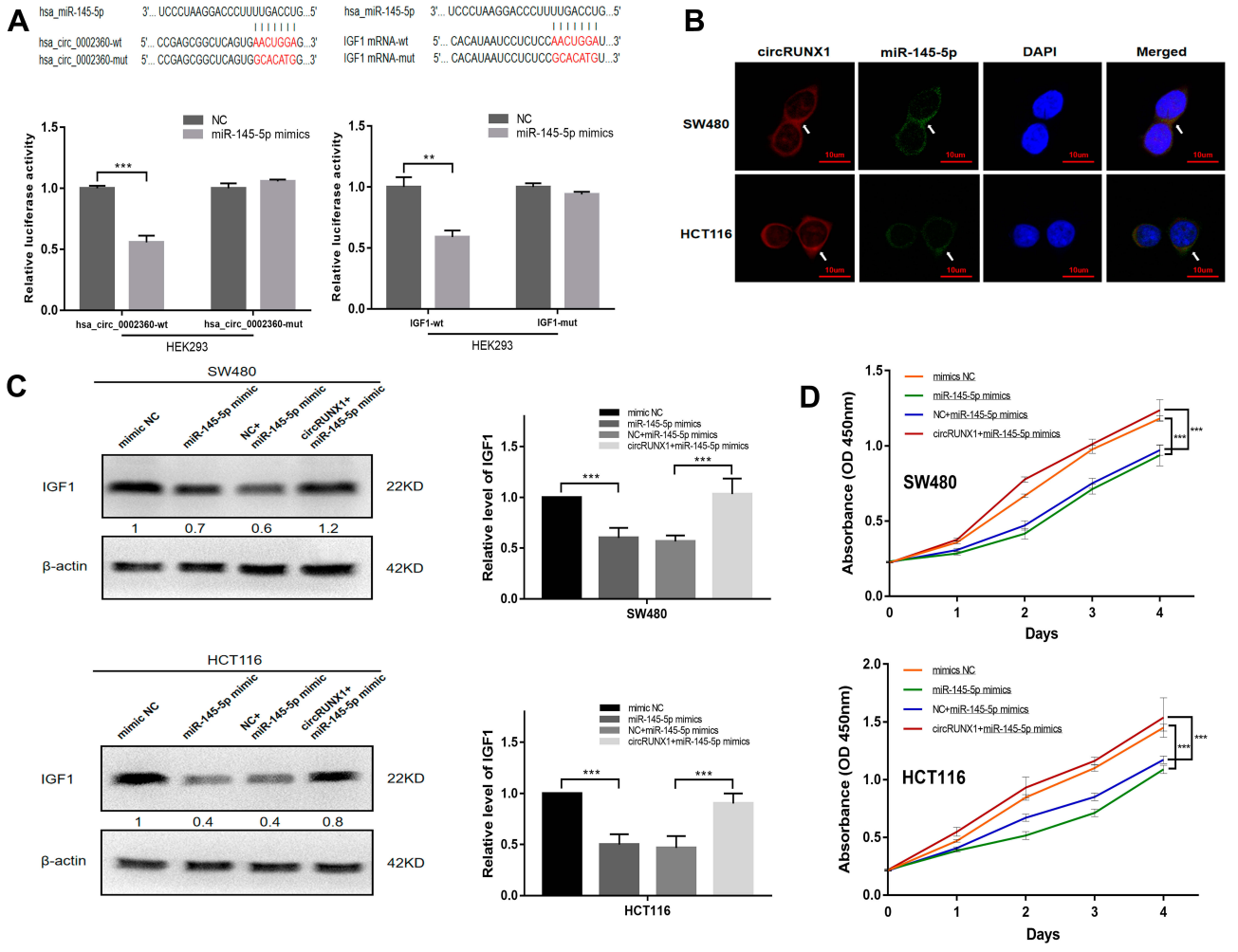

Figure 7 circRUNX1 facilitated cell proliferation by relieving repression of miR-145-5p for IGF1 expression. (**A**) Schematic of the predicted miR-145-5p binding site in circRUNX1 and mutant binding site. Dual-luciferase reporter assay showed a significant decrease of luciferase activity of the vector containing the wild-type (wt) miR-145-5p binding site within circRUNX1, while the luciferase activity was restored with the vector containing mutant (mut) binding site (left). Luciferase reporter assay of wt and mut binding site of IGF1 (right). The relative luciferase activities were normalized with Renilla luciferase activity. (**B**) RNA FISH for circRUNX1 and miR-145-5p in SW480 and HCT116 cells. (**C**) IGF1 expression in SW480 and HCT116 cells transfected with miR-145-5p mimics alone or cotransfected with circRUNX1. (**D**) Cell proliferation analysis for SW480 and HCT116 cells transfected with miR-145-5p mimics alone or cotransfected with circRUNX1. Data are listed as means ± SD of at least three independent experiments. $^{**}p< 0.01$, $^{***}p< 0.001$. Scale bars = 10 μm.

observed significant changes in IGF1 expression between the experimental and control groups. It is hypothesized that IGF1 is a key downstream target of circRUNX1 in the promotion of CRC cell proliferation.

IGF1 is highly expressed in various cancers, such as pancreatic cancer,[21] colorectal cancer,[22] gastric cancer,[12] breast cancer,[23] and acute myeloid leukemia.[24] Previous studies have shown that IGF1 promotes tumor cell proliferation by initiating the PI3K/Akt signaling pathway, which has a great influence on cell cycle, cell migration and angiogenesis in several cancer types including CRC.[25,26] In gastric cancer, the IGF1/IGF1R pathway is involved in the upregulation of STAT3 expression.[12] At the cellular level, action of IGF1 is strictly regulated by IGFBP3, for the affinity of IGF1 to IGFBP3 is higher than that to IGF receptors. Consequently, the protein level of IBGBP3 directly controls the bioavailability of IGF1 to the IGF receptors and thereby indirectly modulates cell proliferation.[24,27] In addition, IGF1 secretion is regulated by GH levels in CRC.[28] However, according to our human growth factor array data, no significant changes in protein levels were detected in IGFBP3 or GH between the experimental and control groups. Based on these findings, we strongly hypothesize that in CRC cells, circRUNX1 is involved in IGF1-induced proliferation through a new signaling pathway.

The ceRNA hypothesis has proposed that RNA transcripts may construct a complex post-transcriptional regulatory network, in which mRNAs, lncRNAs, and circRNAs share the same miRNA response elements, competing for binding miRNAs, and then regulating expression of each other.[29–32] For instance, circTP63 contains miR-873-3p-binding sites and regulates FOXM1 expression via miR-873-3p in lung squamous cell carcinoma.[19] In CRC, miR-597-5p was verified as the binding target of circ101555 and promotes tumor growth by regulating CSNK1G1.[33] To better explore the molecular mechanism

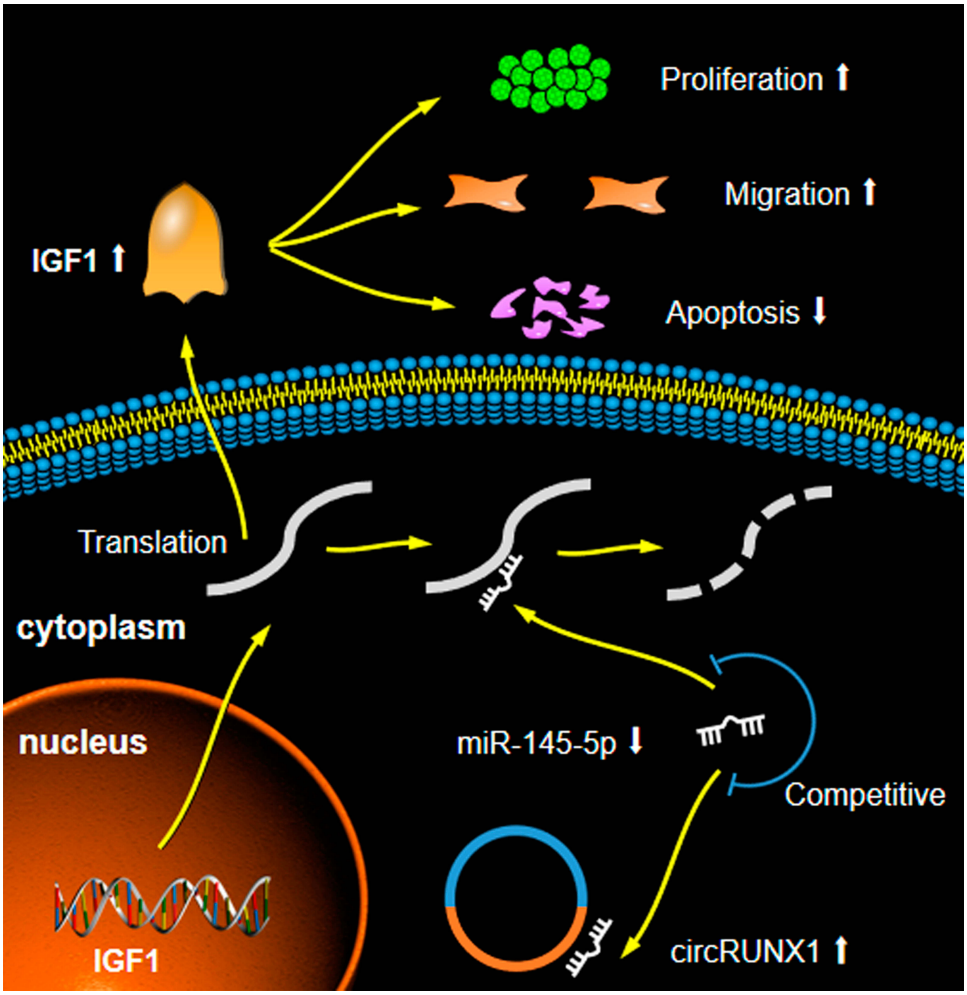

Figure 8 High expression of circRUNX1 decreased level of miR-145-5p, which increased expression of IGF1, thus promoting malignant phenotypes of CRC cells.

of circRUNX1, we used bioinformatics algorithms to predict the miRNA-binding sites. Among these candidates, miR-145-5p was selected as the downstream target of circRUNX1. Reliable evidence showed that miR-145-5p shares the same binding sites with IGF1.[17]

MicroRNAs (miRNAs) are a new class of short non-coding RNAs in tumor biology that can negatively regulate the expression of many target genes by interacting with the 3′ UTR.[34] miR-145-5p was downregulated in CRC and positively associated with poorer overall survival, according to TCGA database.[35,36] Our study showed that miR-145-5p reduced the luciferase activity of circRUNX1 luciferase reporter by almost 50%. FISH assay confirmed the colocalization of circRUNX1 and miR-145-5p. Importantly, our Western blotting analysis strongly indicated that circRUNX1 was the upstream molecule of miR-145-5p, and regulated IGF1 as a ceRNA of miR-145-5p. Cell phenotypes also confirmed overexpression of circRUNX1 could rescue miR-145-5p mimic-mediated suppression for proliferation, implying that miR-145-5p is an essential regulator in this model.

Conclusions

In summary, our work is the first to reveal that circRUNX1 is upregulated in CRC and acts as a tumor promotor that modulates cell proliferation, apoptosis, cell cycle, and migration. Mechanistically, circRUNX1 competitively binds miR-145-5p to abolish the suppressive effect of miR-145-5p on IGF1. These findings provide an insight into understanding the CRC pathogenesis, and a potential target for CRC treatment.

Abbreviations

circRNAs, circular RNAs; IGF1, insulin-like growth factor 1; CRC, colorectal cancer; RT-PCR, reverse transcription-PCR; FISH, fluorescence in situ hybridization; TNM, tumor-node-metastasis; ncRNAs, non-coding RNAs; RNA-seq, RNA sequencing; ceRNA, competing endogenous RNA; siRNAs, small interfering RNAs; CDS, coding sequence; bp, base pairs; TCGA, The Cancer Genome Atlas.

Ethics Approval and Informed Consent

This study was approved by the Ethics Committee of Beijing Chao-Yang Hospital, Capital Medical University and conducted in accordance with the ethical standards formulated in the Declaration of Helsinki. Written informed consent was obtained from all patients. All animal studies were approved by the Committee on the Ethics of Animal Experiments of Beijing Chao-Yang Hospital Capital Medical University, and were performed in compliance with the Animal Protection Law of the People's Republic of China-2009 for experimental animals. We mentioned this information in the manuscript.

Funding

This study was supported by the Capital Health Development Research Project (2018-1-2032) and 1351 Personnel Training Program of Beijing Chao-Yang Hospital Affiliated to Capital Medical University (CYXZ-2017-09).

Disclosure

The authors declare that they have no competing interests.

References

1. Siegel RL, Miller KD, Jemal A. Cancer statistics, 2019. *CA Cancer J Clin*. 2019;69(1):7–34. doi:10.3322/caac.21551
2. Allemani C, Weir HK, Carreira H, et al. Global surveillance of cancer survival 1995-2009: analysis of individual data for 25 676 887 patients from 279 population based registries in 67 countries (CONCORD-2). *Lancet*. 2015;385:977–1010. doi:10.1016/S0140-6736(14)62038-9
3. Fromm B, Domanska D, Høye E, et al. MicroRNA expression reflects site specificity of metastatic colorectal cancer. *Cancer Res*. 2017;77:13. doi:10.1158/1538-7445.AM2017-3432
4. Weng W, Wei Q, Toden S, et al. Circular RNA ciRS-7-A promising prognostic biomarker and a potential therapeutic target in colorectal cancer. *Clin Cancer Res*. 2017;23:3918–3928. doi:10.1158/1078-0432.CCR-16-2541
5. Kristensen LS, Hansen TB, Venø MT, Kjems J. Circular RNAs in cancer: opportunities and challenges in the field. *Oncogene*. 2018;37:555–565. doi:10.1038/onc.2017.361
6. Bach DH, Lee SK, Sood AK. Circular RNAs in cancer. *Mol Ther Nucleic Acids*. 2019;16:118–129. doi:10.1016/j.omtn.2019.02.005
7. Jeck WR, Sharpless NE. Detecting and characterizing circular RNAs. *Nat Biotechnol*. 2014;32(5):453–461. doi:10.1038/nbt.2890
8. Wilusz JE, Sharp PA. A circuitous route to noncoding RNA. *Science*. 2013;340(6131):440–441. doi:10.1126/science.1238522
9. Shang Q, Yang Z, Jia R, Ge S. The novel roles of circRNAs in human cancer. *Mol Cancer*. 2019;18(1):6. doi:10.1186/s12943-018-0934-6
10. Pamudurti NR, Bartok O, Jens M, et al. Translation of CircRNAs. *Mol Cell*. 2017;66(1):9–21. doi:10.1016/j.molcel.2017.02.021
11. Pollak MN, Schernhammer ES, Hankinson SE. Insulin-like growth factors and neoplasia. *Nat Rev Cancer*. 2004;4(7):505–518. doi:10.1038/nrc1387
12. Xu L, Zhou R, Yuan L, et al. IGF1/IGF1R/STAT3 signaling-inducible IFITM2 promotes gastric cancer growth and metastasis. *Cancer Lett*. 2017;393:76–85. doi:10.1016/j.canlet.2017.02.014
13. Werner H. Tumor suppressors govern insulin-like growth factor signaling pathways: implications in metabolism and cancer. *Oncogene*. 2012;31(22):2703–2714. doi:10.1038/onc.2011.447
14. Slattery ML, Samowitz W, Curtin K, et al. Associations among IRS1, IRS2, IGF1, and IGFBP3 genetic polymorphisms and colorectal cancer. *Cancer Epidemiol Biomarkers Prev*. 2004;13:1206–1214. doi:10.1142/S0217751X09043675

15. Li Z, Pan W, Shen Y, et al. IGF1/IGF1R and microRNA let-7e down-regulate each other and modulate proliferation and migration of colorectal cancer cells. *Cell Cycle*. 2018;17(10):1212–1219. doi:10.1080/15384101.2018.1469873
16. Li XN, Wang ZJ, Ye CX, Zhao BC, Li ZL, Yang Y. RNA sequencing reveals the expression profiles of circRNA and indicates that circDDX17 acts as a tumor suppressor in colorectal cancer. *J Exp Clin Cancer Res*. 2018;37:325. doi:10.1186/s13046-018-1006-x
17. Mosakhani N, Guled M, Leen G, et al. An integrated analysis of miRNA and gene copy numbers in xenografts of Ewing's sarcoma. *J Exp Clin Cancer Res*. 2012;31:24. doi:10.1186/1756-9966-31-24
18. Ebbesen KK, Kjems J, Hansen TB. Circular RNAs: identification, biogenesis and function. *Biochim Biophys Acta*. 2016;1859:163–168. doi:10.1016/j.bbagrm.2015.07.007
19. Cheng Z, Yu C, Cui S, et al. circTP63 functions as a ceRNA to promote lung squamous cell carcinoma progression by upregulating FOXM1. *Nat Commun*. 2019;10:3200. doi:10.1038/s41467-019-11162-4
20. Yang H, Xia L, Chen J, et al. Stress-glucocorticoid-TSC22D3 axis compromises therapy-induced antitumor immunity. *Nat Med*. 2019;25:1428–1441. doi:10.1038/s41591-019-0566-4
21. Kopantseva MR, Usova E, Mikaelyan A, et al. Effect of IGF1 on cancer and stromal cells of human pancreatic tumors. *Cancer Res*. 2015;75:15. doi:10.1158/1538-7445.AM2015-1540
22. Yuan L, Zhou C, Lu Y, et al. IFN-γ-mediated IRF1/miR-29b feedback loop suppresses colorectal cancer cell growth and metastasis by repressing IGF1. *Cancer Lett*. 2015;359(1):136–147. doi:10.1016/j.canlet.2015.01.003
23. Zou Y, Zheng S, Xiao W, et al. circRAD18 sponges miR-208a/3164 to promote triple-negative breast cancer progression through regulating IGF1 and FGF2 expression. *Carcinogenesis*. 2019:Pii:bgz071. doi:10.1093/carcin/bgz071.
24. Zhang JM, Wang CC, Zhang GC, et al. ADAM28 promotes tumor growth and dissemination of acute myeloid leukemia through IGFBP-3 degradation and IGF-I-induced cell proliferation. *Cancer Lett*. 2019;442:193–201. doi:10.1016/j.canlet.2018.10.028
25. Wang Y, Mu L, Huang M. MicroRNA-195 suppresses rectal cancer growth and metastasis via regulation of the PI3K/AKT signaling pathway. *Mol Med Rep*. 2019;20:4449–4458. doi:10.3892/mmr.2019.10717
26. Wang G, Lu M, Yao Y, Wang J, Li J. Esculetin exerts antitumor effect on human gastric cancer cells through IGF-1/PI3K/Akt signaling pathway. *Eur J Pharmacol*. 2017;814:207–215. doi:10.1016/j.ejphar.2017.08.025
27. Key TJ, Appleby PN, Reeves GK, Roddam AW; Endogenous Hormones and Breast Cancer Collaborative Group. Insulin-like growth factor 1 (IGF1), IGF binding protein 3 (IGFBP3), and breast cancer risk: pooled individual data analysis of 17 prospective studies. *Lancet Oncol*. 2010;11:530–542. doi:10.1016/S1470-2045(10)70095-4.
28. Soubry A, Il'yasova D, Sedjo R, et al. Increase in circulating levels of IGF-1 and IGF-1/IGFBP-3 molar ratio over a decade is associated with colorectal adenomatous polyps. *Int J Cancer*. 2012;131(2):512–517. doi:10.1002/ijc.26393
29. Salmena L, Poliseno L, Tay Y, Kats L, Pandolfi PP. A ceRNA hypothesis: the Rosetta Stone of a hidden RNA language? *Cell*. 2011;146(3):353–358. doi:10.1016/j.cell.2011.07.014
30. Qi X, Zhang DH, Wu N, Xiao JH, Wang X, Ma W. ceRNA in cancer: possible functions and clinical implications. *J Med Genet*. 2015;52:710–718. doi:10.1136/jmedgenet-2015-103334
31. Miotto M, Marinari E, De Martino A. Competing endogenous RNA crosstalk at system level. *PLoS Comput Biol*. 2019;15:e1007474. doi:10.1371/journal.pcbi.1007474
32. Wang YG, Wang T, Ding M, Xiang SH, Shi M, Zhai B. Hsa_circ_0091570 acts as a ceRNA to suppress hepatocellular cancer progression by sponging hsa-miR-1307. *Cancer Lett*. 2019;460:128–138. doi:10.1016/j.canlet.2019.06.007
33. Chen Z, Ren R, Wan D, et al. Hsa_circ_101555 functions as a competing endogenous RNA of miR-597-5p to promote colorectal cancer progression. *Oncogene*. 2019;38(32):6017–6034. doi:10.1038/s41388-019-0857-8
34. Calin GA, Rezaeian AH, Khanbabaei H. Therapeutic potential of the microRNA-ATM axis in the management of tumor radioresistance. *Cancer Res*. 2019;Pii:canres.1807.2019. doi:10.1158/0008-5472.CAN-19-1807
35. Schee K, Boye K, Abrahamsen TW, Fodstad Ø, Flatmark K. Clinical relevance of microRNA miR-21, miR-31, miR-92a, miR-101, miR-106a and miR-145 in colorectal cancer. *BMC Cancer*. 2012;12(1):505. doi:10.1186/1471-2407-12-505
36. Shinohara H, Kuranaga Y, Kumazaki M, et al. Regulated polarization of tumor-associated macrophages by miR-145 via colorectal cancer-derived extracellular vesicles. *J Immunol*. 2017;199:1505–1515. doi:10.4049/jimmunol.1700167